

Bird's-eye view safety monitoring for the construction top under the tower crane

Yanke Wang¹, Yu Hin Ng¹, Haobo Liang¹, Ching-Wei Chang¹,
Hao Chen^{1*}

¹Hong Kong Center for Construction Robotics, The Hong Kong University of Science and Technology, Units 808 to 813 and 815, 8/F, Building 17W, Hong Kong Science Park, Pak Shek Kok, New Territories, Hong Kong SAR.

*Corresponding author(s). E-mail(s): danielchen16@hotmail.com;
Contributing authors: yankee.wann@gmail.com;
yhngad@connect.ust.hk; hbliang@ust.hk; ccw@ust.hk;

Abstract

The tower crane is involving more automated and intelligent operation procedure, and importantly, the application of automation technologies to the safety issues is imperative ahead of the utilization of any other advances. Among diverse risk management tasks on site, it is essential to protect the human workers on the workspace between the tower crane and constructed building top area (construction top) from the bird's-eye view, especially with Modular Integrated Construction (MiC) lifted. Also, the camera and Light Detection And Ranging (LiDAR) can capture abundant 3D information on site, which is however yet made the best use. Considering the safety protection for humans and tower cranes, we present an AI-based fully automated safety monitoring system for tower crane lifting from the bird's-eye view, surveilling to shield the human workers on the construction top and avoid cranes' collision by alarming the crane operator. The system achieved a 3D data fusion for localization of humans and MiCs by integrating the captured information from camera and LiDAR. The state-of-the-art methods were explored and implemented into our proposed software pipeline coupled with the hardware and display systems. Furthermore, we conducted an analysis of the components in the pipeline to verify the accuracy and effectiveness of the involved methods. The display and visualization on the real site proved that our system can serve as a valuable safety monitoring toolkit on site.

Keywords: bird's-eye view, deep learning, data fusion, MiC lifting safety monitoring

1 Introduction

Tower cranes are essential on modern construction sites, facilitating the lifting and handling of heavy material. However, safety incidents related to tower cranes still occur frequently even though many governments propose restricted operation rules [1, 2]. According to statistics [3], China recorded nearly 125 tower cranes accidents in a single year, and USA witnessed 129 recorded construction crane accidents between 2011 and 2020. Singapore experienced six crane-related fatalities [4] while there were three fatalities in Hong Kong SAR [3] in the year 2022. How to protect the human operators of tower cranes and workers on the construction site has become an intuitively urgent issue since recent accidents keep occurring and continuing annually as the Occupational Safety and Health Administration of USA reported [5]. Based on the knowledge above, increasing attentions are attracted by the safety monitoring of the tower cranes among a great mount of safety concerns [3, 6–8].

The previous research on the safety monitoring of tower cranes is more focused on monitoring the status of tower crane itself. For example, [9] used the vision-based method to obtain the payload displacement. Internet of Things (IoT) technology was also used in [10] to obtain real-time sensor operation data and dynamic structure of tower cranes. In the work of [11], multisensory technology was applied for monitoring the real-time working status of tower cranes. In addition to monitoring the status of the tower crane itself, more researchers begin to take account the human-centered safety issue into site monitoring task. In such case, the deep learning methods are commonly used in the safety monitoring pipeline. For instance, [6] implemented a You Only Look Once (YOLO)v7 to monitor the working space of the workers. Besides, [7] developed a vision-based pipeline to surveil the activities of the workers under the tower crane, e.g., wearing the helmet (or vest) or not. Moreover, the current safety monitoring of the tower crane is mainly based on images [6, 7], which cannot provide depth information. However, the research about three-dimensional safety monitoring is relatively limited [8]. In terms of viewpoint for safety monitoring, the bird’s eye view is more suitable for the safety monitoring of tower cranes, as the monitoring equipment is commonly installed on or over the tower crane that can cover almost the entire lifting process [12].

Recently, Modular Integrated Construction (MiC) is afoot to predominate the construction site owing to its high efficiency, safety guarantee, productivity, and sustainable pre-fabrication [13]. MiC consists of producing building modules off-site, transporting them to the construction site, and assembling them with minimal on-site activities [14]. Although MiC has numerous benefits, it still carries various risks such as crane breakdown issues, inadequate data coordination, modular installation faults, modular production system failures, manual inspecting, and unwrapping among others [15]. The safety issues are mostly focused on the process of fabrication, with concerns by ‘fracture’ or ‘fall’ as a result of the inherently unstable structure [16] in addition to external environmental and organizational factors [17]. Moreover, because of the large size of MiC, the visual blind area of the lifting is also greatly increased [18]. Therefore, a safety monitoring system aiming to build up a safe and efficient MiC operation workspace for tower cranes is necessary.

After a detailed literature research, we raise the following questions,

- How to define the safety concerns in the case of MiC lifting under the tower crane from a bird’s-eye view?
- How to design an automated MiC safety lifting monitoring system based on the mentioned safety concerns?
- What Artificial Intelligence (AI) methods can be applied to the designed system and how do they perform?
- Whether the proposed system can be installed on the real site?

In response to the questions above, we propose an AI-based 3D automated tower crane safety monitoring system from the bird’s-eye view for MiC lifting. The monitoring area is the area between the constructed building top and the tower crane (“Construction Top” for simplicity). We aim to develop such system and apply it on a real construction site in Hong Kong. The challenges regarding the system development come from 1) the data acquisition is inadequate owing to the dangers presented on site; 2) the hidden dangers in the process of MiC lifting are complex and diverse, and how to define safety and insecurity is difficult; and 3) the accuracy and robustness of monitoring technologies are not guaranteed. To the best of our knowledge, there still not exists a sufficient implementation of fully 3D automated safety monitoring for crane lifting tasks of MiC from bird’s-eye view by using the state-of-the-art AI, especially in the case requiring the integration between camera and Light Detection And Ranging (LiDAR). We summarize our contributions as

- In response to the safety concerns on the MiC site, definitions of what constitutes a safe site were provided;
- A fully automated safety monitoring system for MiC lifting on the construction top (CRCUST_Top), involving hardware and information fusion between camera and LiDAR, was proposed with AI capabilities;
- A CRCUST_Top dataset was collected on the real site for training and testing of the pipeline;
- The CRCUST_Top was applied to the real site, working continuously in a long-term manner for the verification of the pipeline.

The testing and verification results demonstrated that our system was adequate to perform the majority of safety monitoring tasks under our definitions.

The remainder of this paper is structured as follows. Section 2 details the related work about safety monitoring on construction sites. Section 3 introduces system design of the proposed safety monitoring system for the construction top under the tower crane. The implementation and results are described in Section 4, and conclusion is drawn in Section 5.

2 Related work

2.1 MiC-involved safety monitoring

The lifting of MiC is most commonly operated by cranes on site, requiring a larger size and higher workload limit of cranes as well as more experienced site workers. This consequently exposes more challenges to the crane operation. In practice, research on

Table 1: AI methods used in the safety monitoring on site.

Method Type	References	Base Model	Safety Issues (detected targets)	Data Source	Year
	[19]	Conventional image processing and machine learning	Workers	Real-site	2018
	[20]	RetinaNet	Workers	Synthetic	2020
	[21]	Conventional image processing and machine learning	Workers	Real-site and synthetic	2020
	[22]	Mask-RCNN	Workers, hazards	Real-site	2019
	[23]	CenterNet	Load zone	Real-site	2022
Vision-based models	[24]	YOLOv8-seg	Construction machinery and operation surfaces	Real-site	2023
	[25]	YOLOv8	Tower cranes	Real-site	2025
	[26]	F-PointNet	MiC	Synthetic	2023
LiDAR-based models	[27]	Cloth Simulation Filtering (CSF)	Tower cranes, lifting objects	Real-site	2023
	[28]	PointNet++	Tower cranes, buildings	Lab-based	Preprint
	[29]	Conventional image processing and machine learning	Load, obstacle, worker, tower cranes	Real-site	2021
LiDAR-visiaon Fusion	[30]	Unity3D® game engine	Drone	Synthetic	2023
	[8]	Mask R-CNN	Objects, workers, crane truck	Real-site and synthetic	2021

MiC-involved safety monitoring on site needs to consider workforce safety [31], cranes' collision, and material damage. Diverse technologies, e.g., Building Information Models (BIM) [32, 33], IoT [34], digital twin [35], virtual reality [36] have been used in the safety management. The BIM is frequently applied in the risk assessment on site with modular construction [32], e.g., by designing a safer site layout scheme [37, 38] or crane operation planning with higher efficiency and safety [39].

In addition, the BIM technology can also be used with the integration of the other technologies. In [35], researchers considered the payload of the tower crane and used digital twin technology to detect the workers under the fall zone of tower crane lifting MiC with the help of IoT and BIM. [40] analyzed the potential risks in MiC, e.g., clash detection, by inputting the real-time 3D BIM to the virtual and digital environment. Seen from above, more and more pioneers are using more than one technology for the safety management and risk estimation.

2.2 Bird's-eye safety monitoring

Although plenty of safety issues are concerning the construction stakeholders, monitoring the site safety from the bird's-eye view stands out as it provides a unique and compressive understanding of the regarding work place [12]. This type of view can be established via two manners, i.e., a sensing system fixed on the body of the tower crane, and rotating with the crane jib or installed on the Unmanned Aerial Vehicles (UAV). Two types of sensors are usually used, visual sensor and LiDAR. Workers can be detected and tracked visually from bird's-eye view, e.g., [19, 21] did the detection from the view with 15 m above the workers. [22] installed a camera on the trolley of one boom tower crane, capturing the view surrounding the hook for measuring the safety distance between workers and site hazards. [23] used the existing camera installed on the top of tower crane and detected the load zone via vision-based method. [24] achieved the bird's-eye view by using a UAV with 20 m above the tower crane, aiming to monitor construction machinery and operation surfaces on site. Similarly, [25] used a UAV to monitor the movements of multiple cranes on site from the bird's-eye view. The details of the work mentioned above is outlined in Table 1. The AI methods used from the bird's-eye view are discussed in the next section according to the sensors installed in the risk management system.

2.3 AI for the safe site

As mentioned in the Section 2.2, the AI methods are applied according to the used sensor devices, i.e., vision-based and LiDAR-based methods. This section aims to detail the literature research on visually servoing and LiDAR enhanced safety monitoring under cranes as well as the State Of The Arts (SOTA) on the data fusion between vision and LiDAR in the case of bird's-eye view under the tower crane.

2.3.1 Visual servoing safety monitoring

The visual perception on site can be processed via the conventional image processing and machine learning methods or advanced deep learning-based models. In the scenarios with little environmental changes, the conventional image processing works

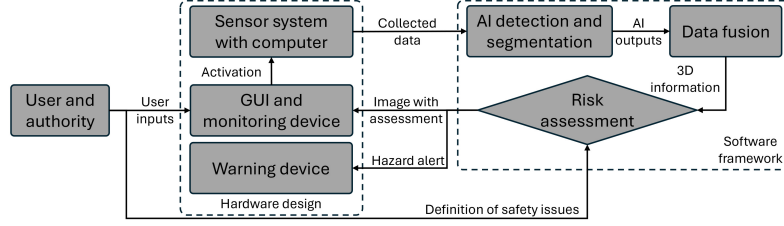


Fig. 1: The workflow of the designed CRCUST-Top, including the components of the hardware design and software framework.

stably and not computationally. For example, [19] analyzed the histogram of the image and difference between two frames as well as Kalman filter for the worker detection and tracking. Moreover, they tested the pipeline both on real-site and synthetic data [21]. These methods usually work in the limited workspace on site and rely on the user-initialized priors, e.g., the image threshold, object size information, target moving speed and range, etc. However, the aforementioned information shows dynamic changes on the real-time workspace, especially on the construction top area. Thus, the deep learning-based methods are potential to show their advantages in handling the changes of image brightness, color, and resolution as well as object scale and moving. The visual deep learning models commonly utilize convolutional neural networks for feature extraction, anchor-based mechanism for object detection, and fully convolutional neural networks for semantic segmentation. [20] followed the architecture of RetinaNet to do the detection of workers under crane from a load-view (similar to bird's-eye view). [22] used Mask-RCNN to predict the area and segments of workers and hazards. [23] adapted a CenterNet to detect the corners of load for defining the working area, and the categories of loads were pre-labeled. [24] improved YOLOv8-seg model for the segmentation of construction machinery and operation surfaces from remote sense images. Although the deep learning-based methods deliver excellent performance, they also suffer from the data issue since these methods require a large-scale dataset size to train a robust and accurate model. Apart from the machines and human workers on site, the safety of tower cranes has also been paid attention. [25] implemented a YOLOv8-based method for the skeleton detection of multiple tower cranes for avoiding the collision between cranes based on the safety distance assessment. The data collection strategy for the work above is also listed in Table 1.

2.3.2 LiDAR enhanced safety monitoring

The computer vision methods are sensitive to the image quality and might suffer from the accuracy for instant warning of risks [35]. Thus, an alternative device generating bird's-eye view is LiDAR. However, only a very limited number of research is focused on the LiDAR-based safety monitoring on site owing to its more challenging data collection procedure than 2D images. In response, [26] offered a well-suited solution to the mentioned question in a virtual world. They simulated the lifting of different types of MiC on site for data generation and selected F-PointNet to do the 3D object detection. [27] designed a LiDAR system to do anti-collision between the lifting objects and

tower crane via a Cloth Simulation Filtering (CSF)-based segmentation. 3D classification can also be used to generate anti-collision warning of tower cranes and buildings [28], where a PointNet++ was applied to laboratory collected data. This section conveys a critical argument that research on bird’s-eye view safety monitoring via LiDAR is limited and still open for further investigation by scholars.

2.3.3 LiDAR-vision fusion

This paper intends to implement the bird’s-eye monitoring of lifting MiC based on the data fusion of 2D image and LiDAR. Only a few research projects are related to this topic. In the context of related research, multiple sensors were integrated together to build a 3D visualization of the site with boom crane in [29]. In that work, the camera was mounted at boom-tip, and a drone-based laser scanning was used to get the mapping of the environment. The above information were combined to generate a complete 3D model of the site. Besides, the boom angle sensor provided the pose estimation of the crane, so the work can fulfill obstacle and worker detection as well as monitor the crane working status. However, the update of the environment is not fully automated, and the drone-based point cloud generation is not real-time, so the application of the research to site with dynamical changes is still limited. Moreover, on the site with multiple drones, the collision between them is also an important safety issue, so [30] simulated 4D drone-based virtual environment to evaluate the effects of flight parameters in risks under different scenarios. Despite not from bird’s eye view, [8] tried to narrow the gap between AI technologies and LiDAR-vision fusion by generating pseudo point cloud data from 2D ground-view image. They modified mask R-CNN for 3D object detection from the generated point clouds and detected collisions between objects (workers) in the work zone of crane truck.

Based on the knowledge above, a research gap is clearly observed. In terms of safe tower crane site with MiC involved, the LiDAR is still not widely used for safety monitoring, neither the LiDAR-vision data fusion. Also, the SOTA of AI technologies still need more exploration and validation on the real site in the scenarios mentioned above. Thus, this study shows its significance by fulfilling the gap and providing the guidance in the regarding research.

3 System design

The objective of the designed system is to monitor the safety issues on the defined construction top workspace under the tower crane. The section provides the detailed solutions to the answers posed in Section 1, with the workflow as Fig. 1 visualizes. The user and authority provides user inputs (system settings, e.g., the thresholds and arguments) and definitions of safety issues according to the governmental regulations. Given the system settings, the Graphical User Interface (GUI) releases activation signal to the sensor system for data acquisition. The collected data are processed by the AI detection and segmentation methods with the outputs used for data fusion. The fused 3D information is then used for a risk assessment guided by the definition of safety issues. The assessed results are interpreted in two manners, i.e., an image with resulting information for a display on the GUI with a monitoring device and an

alert of hazard via a warning device. The details are further discussed in this section, including the definitions of safety issues, coordinate system and pipeline, as well as the hardware and software design and the GUI used for a display.

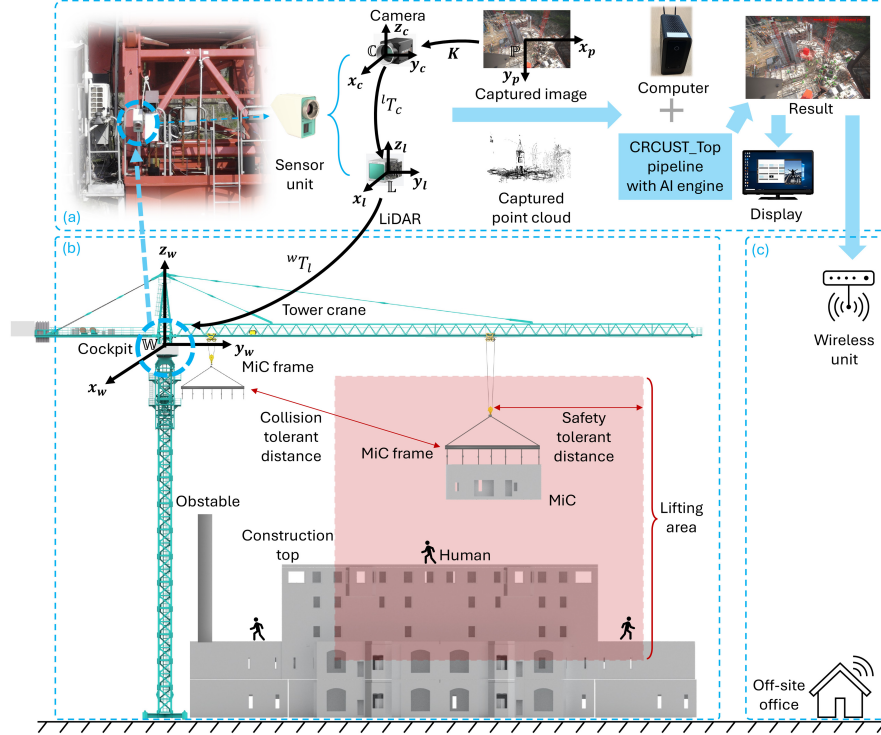


Fig. 2: The diagram showing the hardware design of CRCUST-Top and definition of the safety issues on the construction top. The hardware of the system installed on the cockpit contains a computer, a display, a sensor unit, and a wireless unit connecting with the off-site office. The safety issues include the protection of the humans presenting in the lifting area near to MiC on the construction top and avoidance of MiC frames' collision (cranes' collision).

3.1 Concept

As not too much recent safety management research has involved the safety monitoring of MiC lifting from bird's-eye view. The application of AI in the LiDAR-vision fusion is not explored thoroughly. Thus we provide a few frequently-referred definitions for the easy design of the CRCUST-Top as well as the potential guidance to the future related work.

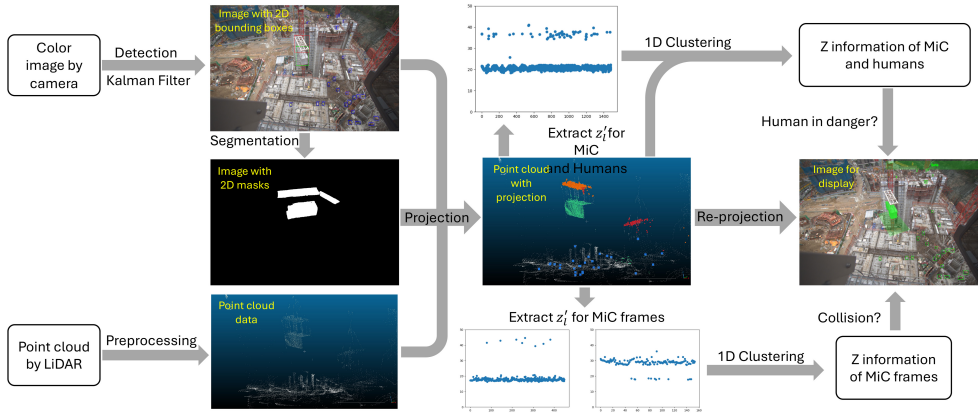


Fig. 3: The software pipeline of CRCUST_Top. The color image captured by the camera is processed by detection method and Kalman filter to obtain the 2D bounding boxes of humans, MiC and MiC frames, followed by a segmentation for 2D masks of them. The Point Cloud (PC) data by LiDAR are fused with the segmentation and detection results for projecting the 2D information to 3D and extracting z_i^l by using one-dimensional clustering. The collected 3D information is re-projected to 2D and display the potential hazards.

3.1.1 Safety definition and challenges

Defining the safety requirements is complex, and it is challenging to consider an all-encompassing guarantee of the construction operators' safety, especially on the construction top during the lifting of the MiC. MiC is a free-standing construction component that is delivered from the prefabrication factory to the construction site [41], ensuring an efficient and solid construction manner. The lifting of the MiC by tower crane is characterized as

- the same starting point of the lifting operation for each building,
- the consistent genres of MiC throughout all construction process, and
- different types of MiC constructed with the similar structure or material.

The autonomous lifting of MiC is therefore attracting the attention of the construction industry. According to the visualization in Fig. 2 (b), we define the space between the tower crane and constructed building as the construction top, where the humans operate and finish the installation of MiCs. The lifting is achieved by the tower crane with a MiC frame and the space around the MiC with a predefined safety tolerant distance is denoted as lifting area. Herein we propose two important safety issues, i.e., protection of the humans under MiC or aside given the safety tolerant distance and avoidance of the collision between the obstacles, MiC frames, and cranes given a collision tolerant distance. In spite of other potential safety threatens, we choose these two issues in response to the most concerns from the construction industry.

3.1.2 Coordinate system

For explicit mathematical representations of the pipeline, as visualized in Fig. 2 (a) and (b), four coordinate systems are defined for CRCUST_Top, including the world coordinate system \mathbb{W} , LiDAR coordinate system \mathbb{L} , camera coordinate system \mathbb{C} , and pixel coordinate system \mathbb{P} . The coordinates in the coordinate systems can be transformed mutually via the transformation matrixes, i.e., wT_l from \mathbb{L} to \mathbb{W} , lT_c from \mathbb{C} to \mathbb{L} , and K from \mathbb{P} to \mathbb{C} (known as intrinsic matrix). \mathbb{W} and \mathbb{L} share the same origin and wT_l only consists of a rotation matrix, i.e., ${}^wT_l = \begin{bmatrix} {}^wR_l & 0 \\ 0 & 1 \end{bmatrix}$. A pixel in \mathbb{P} , $[x_p, y_p, 1]^T$, can be transferred to a point in \mathbb{W} , $[x_w, y_w, z_w]^T$, as follows,

$$\begin{aligned} \begin{bmatrix} x_w \\ y_w \\ z_w \\ 1 \end{bmatrix} &= {}^wT_l \begin{bmatrix} x_l \\ y_l \\ z_l \\ 1 \end{bmatrix} = {}^wT_l {}^lT_c \begin{bmatrix} x_c \\ y_c \\ z_c \\ 1 \end{bmatrix}, \\ \begin{bmatrix} x_c \\ y_c \\ z_c \end{bmatrix} &= K \begin{bmatrix} x_p \cdot z_c \\ y_p \cdot z_c \\ z_c \end{bmatrix} = \begin{bmatrix} f_x & 0 & c_x \\ 0 & f_y & c_y \\ 0 & 0 & 1 \end{bmatrix} \begin{bmatrix} x_p \cdot z_c \\ y_p \cdot z_c \\ z_c \end{bmatrix} \end{aligned} \quad (1)$$

where f_x, f_y are the scaled focal length in x and y axis respectively, c_x, c_y are the pixel translation in x and y axis respectively, and z_c is unknown by the image in \mathbb{P} . Therefore, the CRCUST_Top pipeline needs to involve the search of z_c , as detailed in Section 3.3.1. According to the defined safety concerns in Section 3.1.1, the positions of MiCs, MiC frames, and humans at each timestamp in \mathbb{W} are to be localized for a real-time safety monitoring based on our pipeline.

3.1.3 Point cloud angle distance

A 2D point in the image space (\mathbb{P}) corresponds to a vector in the Point Cloud (PC) data space (\mathbb{L}). In the process of LiDAR-vision data fusion, it is necessary to find the closest 3D point in \mathbb{L} to this vector. Thus, we introduce an angle distance metric to measure their distance. Let $\overline{O_l S_l}$ represent the projected vector in \mathbb{L} from a 2D image point in \mathbb{P} , the target closet point to $\overline{O_l S_l}$ is denoted as M_l , and M_{li} is one of the candidate 3D closest points in PC data space (\mathbb{L})¹. The details are shown in Fig. 4, where two auxiliary lines are defined, i.e., $\overline{O_l S_l}$ (from the origin O_l to the point S_l) and $\overline{O_l M_{li}}$ (from O_l to the point M_{li}). The interior angle θ_i between these two lines is defined as the angle distance between $\overline{O_l S_l}$ and M_{li} . Consequently, the point M_{li} with the lowest angle distance, i.e., M_l , indicates the closest point to $\overline{O_l S_l}$ in \mathbb{L} .

¹The definition of angle distance metric is used to measure the distance between a vector $\overline{O_l S_l}$ and a point M_{li} in \mathbb{L} , which is to be used in the search of z'_l as mentioned in Section 3.3.1.

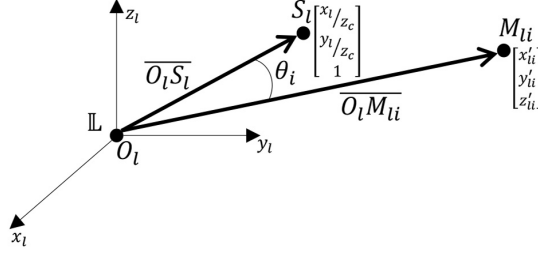


Fig. 4: The diagram explaining the definition of point cloud angle distance, as mentioned in Section 3.1.3. $\overline{O_l S_l}$ is the projected vector in \mathbb{L} from a 2D image point in \mathbb{P} , and M_{li} is a 3D point in \mathbb{L} .

3.2 Hardware design

3.2.1 Components of hardware

The hardware system of CRCUST_Top contains a host computer (ZOTAC MINI PC ERP74070C), a display monitor, a wireless internet module, and a sensor unit with two sensors, i.e., a remote camera (MV-CS200-10GC) and a LiDAR (Livox AVIA with a built-in Inertial Measurement Unit (IMU)), as visualized in Fig. 2. The devices are installed to rotate together with the crane cockpit, ensuring a possible 360-degree view of the construction top space. Importantly, the host computer processes the captured data by the sensor unit locally by using intelligent workflow (discussed in Section 3.3). The real-time monitoring status of the tower crane operation is displayed in the cockpit for the crane driver. Also, the resulting output is transmitted to the off-site office via wireless internet module for backup and guarantee, thereby releasing the data burden between on-site and off-site devices of the CRCUST_Top.

3.2.2 LiDAR-camera calibration

The LiDAR-vision data fusion aims to achieve the information transformation between image collected by camera and PC collected by LiDAR. The calibration between them is the key to the task, including the intrinsic (K) and extrinsic (lT_c) calibrations. The calibration procedure of intrinsic follows the toolbox [42, 43], which is conducted prior to the calibration of extrinsic transformation matrixes. As the LiDAR used in the system integrates a IMU that provides the rotation of the LiDAR with respect to \mathbb{W} . Therefore, only lT_c needs calibrating in our system. We execute the extrinsic calibration according to [44] which conducts the LiDAR-camera calibration in the pixel level².

3.3 Software design

3.3.1 Software framework

Considering the fusion of the two sensors as well as making the pipeline easy-to-use, we apply a two-dimensional (2D) detection method in the working flow, shown as

²Extrinsic calibration: https://github.com/hku-mars/livox_camera_calib.

Fig. 3. Given the image captured by the camera, the detection method generates 2D bounding boxes, including MiC and MiC frame lifted by the tower crane and humans on the construction top. As the detection has the possibility missing the objects, a post-processing step is added according to the previous detection results. Herein we use a Kalman filter [45] to conduct this task since we assume the moving of MiC is stable by the tower crane. Besides, the 2D bounding boxes of MiC and MiC frame may also contain the information of other instances in the scenarios. A segmentation is used to generate a mask of MiC within the 2D bounding box area. On the other hand, the PC data is captured by LiDAR for gathering the third-dimensional information of the objects. We apply the preprocessing (down-sampling and zero-value removal) to the original PC data that contains a great amount of redundant points. The 2D bounding boxes of humans and segmentations of MiC and MiC frame in \mathbb{P} are projected to \mathbb{W} given the calibrated intrinsic metric (K) of the camera and extrinsic transformations (${}^lT_c, {}^wT_l$) as described in Section 3.1.2. In this work, we let the term “Projection” indicate that a point is transferred from pixel coordinate system \mathbb{P} to world coordinate system \mathbb{W} , and re-projection vice versa. In response to the problem proposed in Section 3.1.2, i.e., z_c yet determined, we rewrite lT_c as

$${}^lT_c = \begin{bmatrix} {}^lR_c & {}^lt_c \\ 0 & 1 \end{bmatrix} = \begin{bmatrix} r_{11} & r_{12} & r_{13} & t_x \\ r_{21} & r_{22} & r_{23} & t_y \\ r_{31} & r_{32} & r_{33} & t_z \\ 0 & 0 & 0 & 1 \end{bmatrix} \quad (2)$$

and Eq. 1 as

$$\frac{x_c}{z_c} = f_x x_p + c_x, \quad \frac{y_c}{z_c} = f_y y_p + c_y \quad (3)$$

$$\frac{z_l}{z_c} = r_{31} \frac{x_c}{z_c} + r_{32} \frac{y_c}{z_c} + r_{33} + t_z = r_{31}(f_x x_p + c_x) + r_{32}(f_y y_p + c_y) + r_{33} + t_z \quad (4)$$

The point $[x_p, y_p]^T$ in \mathbb{P} is transferred to “scaled point” $[\frac{x_c}{z_c}, \frac{y_c}{z_c}, 1]^T$ in \mathbb{C} , denoted as S_c , and then to $[\frac{x_l}{z_c}, \frac{y_l}{z_c}, 1]^T$ in \mathbb{L} , denoted as S_l . We define a line from the origin of \mathbb{L} to S_l , denoted as $\overline{O_l S_l}$, and the search of z_c is conducted along with $\overline{O_l S_l}$. Although the 2D image cannot provide the third-dimensional information, LiDAR provide 3D positions in \mathbb{L} , and owing to the feature of scanning mode used by LiDAR, only one 3D point is present in each direction [46]. Thus, an intuitive way searching z_c is to find the closest point, defined as $M_l, [x'_l, y'_l, z'_l]^T$ to the line $\overline{O_l S_l}$ in \mathbb{L} . Specifically, the closest point M_l indicates the line $\overline{O_l M_l}$ between the origin and M_l has the smallest interior angle distance with $\overline{O_l S_l}$. More details are described in Section 3.1.3. According to the find of M_l and corresponding S_l , z_c is calculated by solving

$$\frac{z'_l}{z_c} = r_{31}(f_x x_p + c_x) + r_{32}(f_y y_p + c_y) + r_{33} + t_z \quad (5)$$

since $r_{31}(f_x x_p + c_x) + r_{32}(f_y y_p + c_y) + r_{33} + t_z$ is known given a specific point $[x_p, y_p]^T$ in \mathbb{P} and transformation matrices (lT_c and K). As only one closest point M_l is selected

to compute z_c , possibly with inaccuracy caused by LiDAR error, we propose to use all possible points, denoted as $\{M_{li}\}_{i=0,1,2,\dots}$, in \mathbb{L} by transferring all the pixels within segments in \mathbb{P} to \mathbb{L} , and apply a one-dimensional clustering on all the possible M_{li} to obtain a more accurate z_c . As details visualized in Fig. 3, z_c values for humans, MiC, and MiC frames are clustered and transformed to the camera coordinate to ascertain x_c, y_c . Based on the 3D information above that is to be transferred to W , the dangers are diagnosed by

- comparison between the detected humans and MiC for finding the presence of humans in danger, and
- comparison between the detected MiC frames for exploring the dangers of collision between two lifting processes.

Based on the fixed hardware design, the performance of the system mainly relies on the detection and segmentation method, especially for the different types of MiCs and humans in a tiny size. Thus, we consider comparing different SOTA to find the suitable methods and modify them to our pipeline.

3.3.2 Methods used in the framework

The section details the choice of the methods for the CRCUST_Top pipeline. The base of a detection method consists of the feature extraction backbone and bounding box generation head. This work explores the application of YOLO-structure [47, 48] in the detection of large (MiC and MiC frame) and tiny objects (human) simultaneously, as such neural network exhibits strong performance in detection while meeting the real-time requirements. The samples of these objects are unbalanced, i.e., numerous humans and a few MiCs (MiC frames). Therefore, both YOLOv5 and YOLOv8 are compared for selecting a sufficient model, as the Distributed Focal Loss (DFL) used in YOLOv8 aims to solve the imbalance existing in the data. Besides, a segmentation model is added to fine-tune the detection result, and herein we use the Segment Anything Model (SAM) [49] to conduct the 2D segmentation by inputting the 2D bounding boxes from YOLO-based detection as the prompt of SAM. In terms of 3D information processing, two clustering methods, K-Means [50] and Mean-Shift [51], are compared to be used in our pipeline. More comparison and selection of the mentioned models are further discussed in Section 4.

3.4 Graphical user interface

The proposed CRCUST_Top pipeline naturally needs a display (GUI) to warn the crane operators or other personnel on site when dangers occur, as layout in Fig. 5. The GUI presents three components, real-time display of the safety monitoring, essential information regarding safety issues, and control buttons. We display the safe timestamps in green and dangerous timestamps in red with a warning message and alarm. The button contains start and stop of the system plus photo and video capturing capability for back up. Also, the number of MiC and human workers presented in each frame are listed meanwhile.

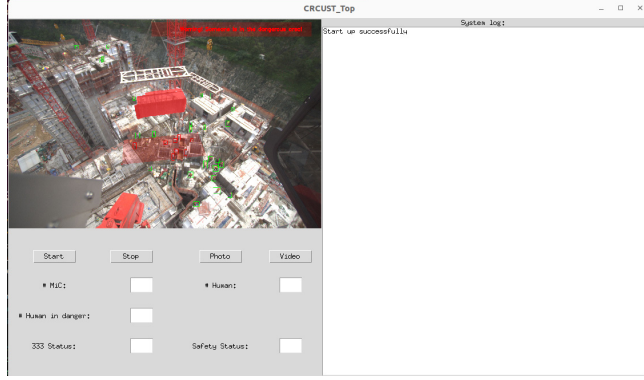


Fig. 5: The GUI of CRCUST_Top, with the real-time display of the safety monitoring, control buttons, and system information logs.

4 Implementation and results

Given the detailed description of the system design, this section explains the parameters used in the system, method implementation, data collection, model training and comparison, ablation study, as well as results and discussion.

4.1 Data collection and training

For our specific detection task, a customized dataset is one of the core challenges for the pipeline. As 3D information is utilized in the CRCUST_Top pipeline as visualized in Fig. 3, images and PC data were gathered in pairs to prepare our dataset. With the installation of the hardware system (more details in Section 3.2.1), we collected 858 image-PC pairs for lifting 5 different types of MiCs and labeled 3 classes in each image, named as CRCUST_Top dataset, and the statistics of the dataset are outlined in Table 2. All data in the dataset were collected on a real site (Public Housing Developments at constructions sites R2-6 and R2-7 on Anderson Road Quarry, Hong Kong SAR.) We split the dataset into train (482 images embodying 11388 human workers, 472 MiCs, and 593 MiC frames) and test (376 images presenting 10673 humans workers, 312 MiCs, and 505 MiC frames) sets. Different categories of the MiCs were considered in train and test sets to examine the generalizability of the detection models. Also, the resolution of the images and sampling ability of the LiDAR are summarized in Table 2, with further details describing the sizes of the bounding boxes of humans, MiCs, and MiC frames shown in the images. The statistics mentioned above present three challenging facts in the pipeline in terms of the related objects, i.e., imbalance of the number, diversities of the sizes, and changing scales of the same class. To this end, the employed method is required to migrate the problems for fulfilling a sufficient pipeline on the construction site. The training of the detection models was executed on the computer (AMD®Ryzen 9 5959x) with a RTX4090 D X3 24GB until the convergence of the models, and as mentioned in Section 3.2.1, the host computer used in on the real site has an i7-14700 processor with a RTX4070 Super 12 GB. The average time

of computation used for each frame is 1.639 s, including detection, segmentation, projection, and visualization.

Table 2: The statistics of the CRCUST_Top dataset.

Split	Train	Test	
Number of pairs: images and point clouds	482	376	
Number of humans	11388	10673	
Number of MiCs	472	312	
Number of MiC frames	593	505	
Image resolution (width \times height, pixels)	5472×3648		
Number of points for each PC frame	24000		
	Human	73.83×91.29	73.76×88.47
	MiC	467.16×702.14	394.18×427.47
	MiC frame	592.11×639.40	789.87×446.50
Average size of bounding boxes: width \times height (pixels)			

4.2 Evaluation metric

Two groups of methods need comparisons for the selection of the models, i.e., detection model and one-dimensional clustering, so we considered mean Average Precision (mAP) [52] and distance error (*err*). The definition of mAP is based on the Intersection over Union (IoU) that measures the positional similarity of two bounding boxes. Given two bounding boxes, B_p (prediction) and B_g (ground-truth), the IoU between them is computed as

$$IoU = \frac{A(B_p \cup B_g)}{A(B_p \cap B_g)} \quad (6)$$

where $A(B_p \cup B_g)$ is the area of the overlap between B_p and B_g , and $A(B_p \cap B_g)$ is the area of the union between B_p and B_g .

The precision (P) and recall ratio of an object detection model can be computed as

$$P = \frac{TP}{TP + FP} \Big|_{T_{IoU}, T_c} \quad (7)$$

$$R = \frac{TP}{TP + FN} \Big|_{T_{IoU}, T_c} \quad (8)$$

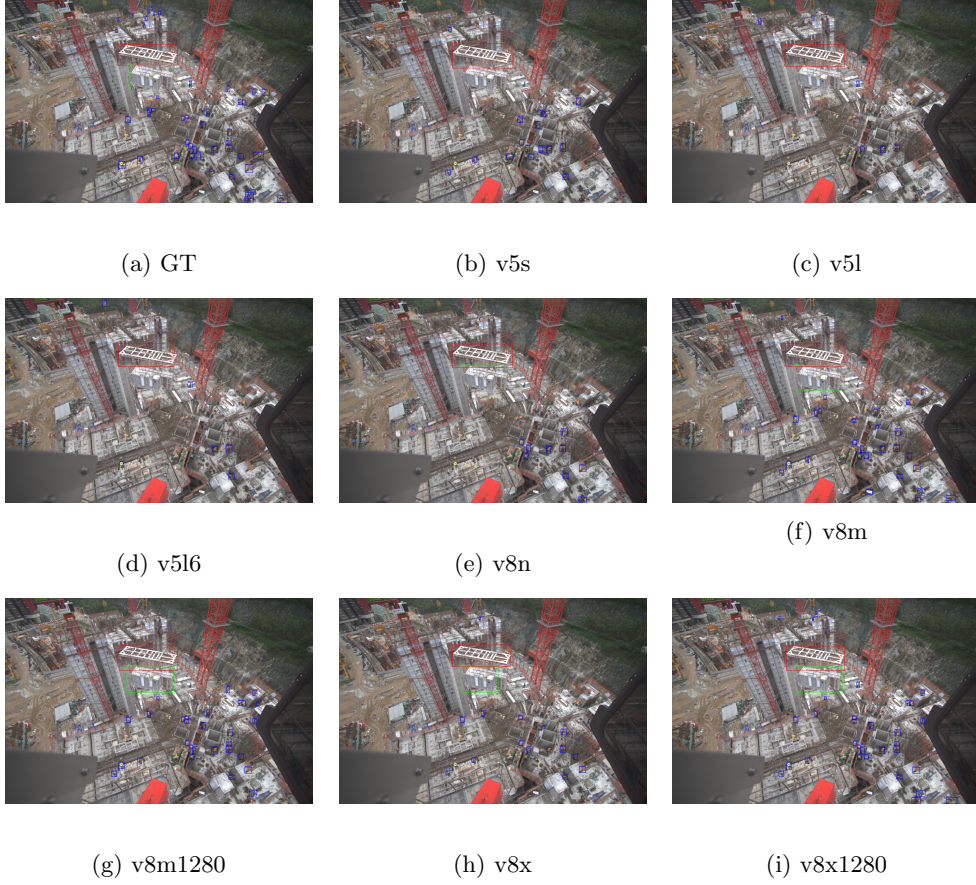


Fig. 6: The comparison of the detection results by YOLOv5 and YOLOv8 with IoU threshold = 0.3, Confidence threshold = 0.5 (humans), and Confidence threshold = 0.7 (MiCs and MiC frames).

where TP, FP, and FN indicate

- True Positive (TP): the correct detection with confidence value over T_c , i.e., its IoU with corresponding ground truth over a threshold T_{IoU} ;
- False Positive (FP): the incorrect detection with confidence value over T_c , i.e., its IoU with wrongly matched ground truth over a threshold T_{IoU} ;
- False Negative (FN): the undetected ground-truth with confidence value over T_c , i.e., its IoU with all detection lower than T_{IoU} .

In practice, P and R can be displayed as a trade-off curve given different T_c . Average Precision (AP) is usually used to combine these two indexes by integrating the curve from $T_c = 0$ to $T_c = 1.0$. Moreover, mAP is the mean of AP over all classes in dataset. We use two values (50% and 95%) of T_{IoU} to test the model, i.e., mAP50 and mAP95.

Additionally, we aim to measure the localization accuracy in 3D, so the error distance between two 3D points is computed as

$$err = \sqrt{(x' - x_g)^2 + (y' - y_g)^2 + (z' - z_g)^2} \quad (9)$$

where $\{x', y', z'\}$ is the predicted point, and $\{x_g, y_g, z_g\}$ is the ground-truth point.

4.3 Comparison of detection models

Although the SOTA of the detection methods have emerged as a success, many challenges in our safety case cannot still be solved. Thus, 6 YOLOs were compared on our customized data by using the mAP50 and mAP50-95 (the higher the better), as visualized in Table 4 and in Fig. 6. Among them, two image sizes (640 and 1280) were considered in YOLOv8m and YOLOv8x. The results delivered that YOLOv8x outperformed the other models in most indexes, especially in image size at 1280. Nonetheless, the size of the YOLOv8x was almost three times larger than YOLOv8m, which, at the meantime, had comparable accuracy. Therefore, YOLOv8m was taken into account in the pipeline.

4.4 Safety monitoring visualization

The safe monitoring intuitively requires a display for warning the tower crane operator in case of dangers. We simplified the display by using two colors showing safe and dangerous cases of lifting the MiC, i.e., without and with danger during the moving of MiC. As visualized in Fig. 8, the safe case is colored in green (Fig. 8a and 8c) and the dangerous case in red (Fig. 8b and 8d). The 3D area of the MiC was enlarged with a safety tolerance and re-projected back to the mask in the image space. Any human presenting in the mask or collision triggered the warning of dangers. The projection plane was the same as the construction top, where the human operators were working.

4.5 Ablation study

The CRCUST_Top pipeline integrated various methods to take the mutual advantages, so the lack of any specific one can undermine the pipeline’s performance. To verify the functions of the methods involved in the pipeline, we conducted the ablation study for the segmentation part and one-dimensional clustering.

Segmentation A SAM was applied to the detected 2D bounding boxes for generating fine object instance areas of MiC and MiC frame. We compared two projections of the object areas in the 3D PC data, i.e., from masks generated by SAM and from these generated merely by the detection result (2D bounding boxes). As detailed in Fig. 7, the projection with only detection result caused more noise points in PC data, thereby consequently extracted z'_l presenting less obvious clusters, compared with that by SAM. The core function of the SAM was to remove the background area within the mask and then reduced the noise points in terms of extracting z'_l . An accurate z'_l searching can ensure a better localization of the target objects (MiC and MiC frame).

One-dimensional clustering As the third dimensional information of the target objects was essential to the safety monitoring, a proper selection among the abundant

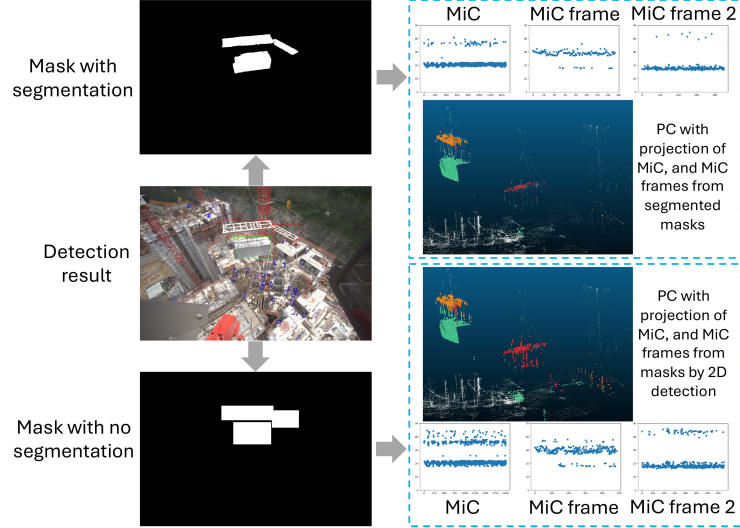


Fig. 7: The comparison for z'_l extraction with and without segmentation. In PC data, MiC points are in green, one MiC frame in yellow, and another in red.

Table 3: The comparison of clustering methods for obtaining z'_l .

Method	Averaging	K-Means	Mean-Shift
<i>err</i> (m)	4.12	1.41	3.58

extracted z'_l by SAM had a decisive role in the 3D localization. We aimed to make the pipeline less computational and easy-to-use, so three simple but sufficient methods were compared in Table 3. In order to evaluate the accuracy of the clustering in our case, 8 objects (MiC and MiC frame) in different PC data from the dataset were randomly selected with the corresponding centers chosen manually as ground truth. We compared the calculation of the 3D localization by three methods, i.e., averaging, K-Means, and Mean-Shift for z'_l , with the ground truth and Table 3 outlines the distance errors (*err*). The K-Means clustering outperformed the others and had less computation than Mean-Shift as well, so it was implemented in our CRCUST_Top pipeline.

4.6 Limitations

This work presents a system for the safety monitoring of construction top, and in most cases, the dangers can be detected and warned, although some limitations need to be noticed. We heuristically selected a higher confidence threshold for MiC and MiC frame detection as the detection method may pick some false positives owing to the

Table 4: The comparison of the YOLOv5 and YOLOv8 regarding model size, mAP50, and mAP50-95.

Model	Batch size	Image size	Model size (params)	mAP50				mAP50-95			
				Human			All	Human			All
				Human	MiC	MiC frame		Human	MiC	MiC frame	
YOLOv5s	16	640	7.2M	0.418	0.218	0.941	0.526	0.128	0.107	0.584	0.273
YOLOv5l	16	640	46.5M	0.541	0.188	0.91	0.546	0.202	0.113	0.657	0.324
YOLOv5l6	16	640	76.8M	0.428	0.128	0.782	0.446	0.154	0.0465	0.446	0.215
YOLOv8n	16	640	3.2M	0.493	0.669	0.951	0.705	0.169	0.425	0.72	0.438
YOLOv8m	16	640	25.9M	0.629	0.83	0.985	0.815	0.237	0.492	0.784	0.504
	2	1280		0.807	0.819	0.986	0.871	0.363	0.523	0.792	0.559
YOLOv8x	16	640	68.2M	0.586	0.851	0.985	0.807	0.213	0.514	0.801	0.509
	2	1280		0.774	0.887	0.992	0.884	0.336	0.599	0.762	0.566

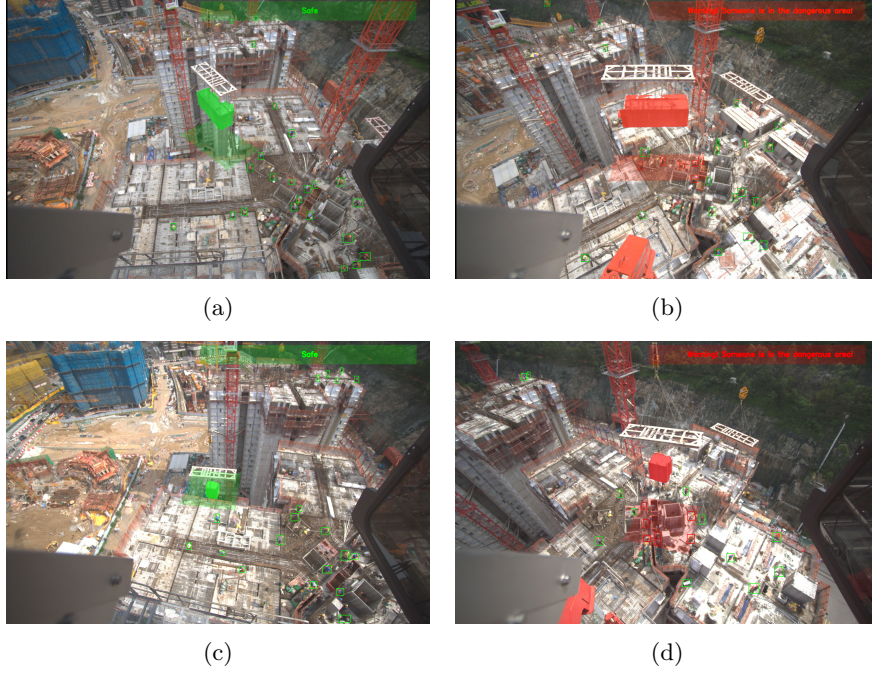


Fig. 8: The visualization of displaying the safe (green) and dangerous (red) cases during the lifting of two types of MiCs.

limited features and similar feature to the surroundings. However, a higher threshold may result in more missing of the detection. Besides, a lower confidence threshold was applied to the human detection for ensuring no missing of possible humans. The center of the bounding box was used as the position of humans, so a small part of the 'fake' detection of human body occurring in the dangerous area may cause the warning, i.e., false positives. Also, even though the object occlusion did not usually occur in our site case, the occlusion with near distance between two objects shall be avoided when users evaluate our system for use. Last but importantly, the inference time of the whole pipeline needs improving for a better real-time display on site, even though it is sufficient for current safety monitoring.

5 Conclusion

In response to the increasing safety concerns on the construction sites, typically those with MiC involved, we introduce four questions regarding the safety monitoring of MiC lifting from bird's-eye view. This work tackles the questions by 1) defining two specific safety concerns for tower crane and workforce on the construction top; 2) designing a CRCUST_Top system that realizes the monitoring of the defined safety concerns with automated warning triggers; 3) fulfilling accurate localization of MiC, MiC frame, and human workers by fusing the SOTA 2D object detection with 3D

PC data collected by LiDAR; 4) installing the proposed system on a real site and collecting a site dataset for verification of the implemented models; 5) additionally, assessing the functions of essential component in the software framework by an ablation study. In summary, CRCUST_Top holds functions of AI-based detection capability, 3D measurements, danger alert, and display, and can be applied to the real site for the safety monitoring task. The results and visualization demonstrated the ability of the pipeline conducting danger detection and warning (display). Subsequently, we aim to research the potential application of open-vocabulary object detection, so that no real-site datasets are necessary, which is usually a highly challenging step in terms of AI application on site. Also, the proposed CRCUST_Top can be relocated to other sites without further modifications, and a commercialization step is under consideration as well, aiming to improve the safety guarantee on more real-world sites.

Acknowledgements. The work was funded by InnoHK-HKCRC. The authors would like to thank the project support from HKCRC Limited and data acquisition support on the construction site from Development and Construction Division, Housing Department, Government of Hong Kong, Hong Kong, China. Additionally, the authors also thank the colleagues, Mr. Zhengyao Liu and Mr. Wanyou Yang, for assisting with the hardware design and figure preparation.

Data availability. Data will be made available on request.

Notes on contributors. Conceptualization and data collection, Y. Wang, Y. H. Ng, H. Liang, C. W. Chang, H. Chen; methodology, experiments, validation, investigation, and visualization, Y. Wang, Y. H. Ng, C. W. Chang, H. Chen; formal analysis and writing—original draft preparation, Y. Wang, H. Chen; writing—review and editing, Y. Wang, Y. H. Ng, C. W. Chang, H. Chen. All authors have read and agreed to the published version of the manuscript.

Declarations. The authors declare no conflict of interest.

References

- [1] WorkSafeBC: New tower crane regulation takes effect oct. 1. Media Relations, WorkSafeBC (2024)
- [2] Academy, S.: Lifting regulations and requirements in singapore for the construction industry. SCAL Academy Pte Ltd (2024)
- [3] Ali, A.H., Zayed, T., Wang, R.D., Kit, M.Y.S.: Tower crane safety technologies: A synthesis of academic research and industry insights. *Automation in Construction* **163**, 105429 (2024)
- [4] Ku, T.K.X., Zuo, B., Ang, W.T.: Robotic tower cranes with hardware-in-the-loop: Enhancing construction safety and efficiency. *Automation in Construction* **168**, 105765 (2024)
- [5] OSHA: Accident search results (2023)

- [6] Pazari, P., Didehvar, N., Alvanchi, A.: Enhancing tower crane safety: A computer vision and deep learning approach. *Engineering Proceedings* **53**(1), 38 (2023)
- [7] Lam, C.P., Lee, Y.N., Ting, C.L., Wong, P.K.-Y., Cheng, J.C., Leung, P.H.: Chapter predictive safety monitoring for lifting operations with vision-based crane-worker conflict prediction (2023)
- [8] Shen, J., Yan, W., Li, P., Xiong, X.: Deep learning-based object identification with instance segmentation and pseudo-lidar point cloud for work zone safety. *Computer-Aided Civil and Infrastructure Engineering* **36**(12), 1549–1567 (2021)
- [9] Gutiérrez, R., Magallón, M., Hernández, D.C.: Vision-based system for 3d tower crane monitoring. *IEEE Sensors Journal* **21**(10), 11935–11945 (2021) <https://doi.org/10.1109/JSEN.2020.3042532>
- [10] Guanghui, H., Xiaowei, L., Xinkui, L., Zhiyong, S.: Research on safety monitoring system of tower crane based on fem and iot. *China Safety Science Journal* **30**(11), 88 (2020)
- [11] Yang, Z.-q., Yang, J., Yuan, E.: Safety monitoring of construction equipment based on multi-sensor technology. In: ISARC. *Proceedings of the International Symposium on Automation and Robotics in Construction*, vol. 37, pp. 677–684 (2020). IAARC Publications
- [12] Higgins, E.: Unlocking workplace potential through a bird’s-eye view and a worm’s-eye view (2023)
- [13] A critical analysis of benefits and challenges of implementing modular integrated construction. *International Journal of Construction Management* (2021) <https://doi.org/10.1080/15623599.2021.1907525> . Publisher Copyright: © 2021 Informa UK Limited, trading as Taylor & Francis Group.
- [14] Ali, A.H., Zayed, T., Hussein, M.: Crane safety operations in modular integrated construction. *Automation in Construction* **164**, 105456 (2024)
- [15] Khan, A.A., Yu, R., Liu, T., Sepasgozar, S., Chen, C.: A systematic review of risks in modular integrated construction practice. 44th AUBEA Conference: Construction Education - Live the Future, 344 (2021)
- [16] Fard, M.M., Terouhid, S.A., Kibert, C.J., Hakim, H.: Safety concerns related to modular/prefabricated building construction. *International Journal of Injury Control and Safety Promotion* **24**(1), 10–23 (2017)
- [17] Song, Y., Wang, J., Liu, D., Guo, F.: Study of occupational safety risks in prefabricated building hoisting construction based on hfacs-ph and sem. *International Journal of Environmental Research and Public Health* **19**(3), 1550 (2022)

- [18] Zhu, A., Zhang, Z., Pan, W.: Crane-lift path planning for high-rise modular integrated construction through metaheuristic optimization and virtual prototyping. *Automation in Construction* **141**, 104434 (2022)
- [19] Neuhausen, M., Teizer, J., König, M.: Construction worker detection and tracking in bird’s-eye view camera images. In: ISARC. Proceedings of the International Symposium on Automation and Robotics in Construction, vol. 35, pp. 1–8 (2018). IAARC Publications
- [20] Sutjaritvorakul, T., Vierling, A., Berns, K.: Data-driven worker detection from load-view crane camera. In: ISARC. Proceedings of the International Symposium on Automation and Robotics in Construction, vol. 37, pp. 864–871 (2020). IAARC Publications
- [21] Neuhausen, M., Herbers, P., König, M.: Synthetic data for evaluating the visual tracking of construction workers. In: Construction Research Congress 2020, pp. 354–361 (2020). American Society of Civil Engineers Reston, VA
- [22] Yang, Z., Yuan, Y., Zhang, M., Zhao, X., Zhang, Y., Tian, B.: Safety distance identification for crane drivers based on mask r-cnn. *Sensors* **19**(12), 2789 (2019)
- [23] Chian, E.Y.T., Goh, Y.M., Tian, J., Guo, B.H.: Dynamic identification of crane load fall zone: A computer vision approach. *Safety Science* **156**, 105904 (2022)
- [24] Bai, R., Wang, M., Zhang, Z., Lu, J., Shen, F.: Automated construction site monitoring based on improved yolov8-seg instance segmentation algorithm. *IEEE Access* (2023)
- [25] Zhang, F., Liu, H., Wang, L., Chen, Z., Zhang, Q., Guo, L.: State awareness and collision risk assessment algorithm for tower crane based on bidirectional inverse perspective mapping and skeleton key points. *Journal of Construction Engineering and Management* **151**(2), 04024205 (2025)
- [26] Xu, J., Pan, W.: Virtual prototyping-enabled pseudo-lidar point cloud dataset for 3d module detection in modular integrated construction. In: The 30th EG-ICE: International Conference on Intelligent Computing in Engineering (04/07/2023-07/07/2023, London) (2023)
- [27] Wang, K., Zhang, W., Chen, H., Liu, H., Hu, Z., Wei, S., Sun, X.: Lidar scanning system and hd map for collision avoidance in tower crane. In: 2023 International Conference on Computer Applications Technology (CCAT), pp. 324–328 (2023). IEEE
- [28] Pei, X., Yin, C.: Active anti-collision warning for tower cranes with 3d deep learning model: Pointnet++. Available at SSRN 4743452 (2024)
- [29] Price, L.C., Chen, J., Park, J., Cho, Y.K.: Multisensor-driven real-time crane

- monitoring system for blind lift operations: Lessons learned from a case study. *Automation in Construction* **124**, 103552 (2021)
- [30] Zhu, Z., Jeelani, I., Gheisari, M.: Physical risk assessment of drone integration in construction using 4d simulation. *Automation in Construction* **156**, 105099 (2023)
 - [31] Mohandes, S.R., Abdelmageed, S., Hem, S., Yoo, J.S., Abhayajeewa, T., Zayed, T.: Occupational health and safety in modular integrated construction projects: The case of crane operations. *Journal of Cleaner Production* **342**, 130950 (2022)
 - [32] Chatzimichailidou, M., Ma, Y.: Using bim in the safety risk management of modular construction. *Safety Science* **154**, 105852 (2022)
 - [33] Darko, A., Chan, A.P., Yang, Y., Tetteh, M.O.: Building information modeling (bim)-based modular integrated construction risk management-critical survey and future needs. *Computers in Industry* **123**, 103327 (2020)
 - [34] Zhai, Y., Chen, K., Zhou, J.X., Cao, J., Lyu, Z., Jin, X., Shen, G.Q., Lu, W., Huang, G.Q.: An internet of things-enabled bim platform for modular integrated construction: A case study in hong kong. *Advanced Engineering Informatics* **42**, 100997 (2019)
 - [35] Li, P., Xie, J., Ding, J., Zhao, Z., Wu, W., Huang, G.Q.: Real-time locating system-enabled digital twin for crane operation safety monitoring on construction sites. In: 2024 IEEE 20th International Conference on Automation Science and Engineering (CASE), pp. 2689–2696 (2024). IEEE
 - [36] Zhang, Z., Pan, W.: Virtual reality supported interactive tower crane layout planning for high-rise modular integrated construction. *Automation in Construction* **130**, 103854 (2021)
 - [37] Zhou, C., Dai, F., Xiao, Z., Liu, W.: Location optimization of tower cranes on high-rise modular housing projects. *Buildings* **13**(1), 115 (2023)
 - [38] Yang, B., Fang, T., Luo, X., Liu, B., Dong, M.: A bim-based approach to automated prefabricated building construction site layout planning. *KSCE Journal of Civil Engineering* **26**(4), 1535–1552 (2022)
 - [39] Bagheri, S.M., Taghaddos, H., Hermann, U.: Automated safety and practicality enhancement of lift plans in modular construction. *Automation in Construction* **168**, 105731 (2024)
 - [40] Zhou, J.X., Shen, G.Q., Yoon, S.H., Jin, X.: Customization of on-site assembly services by integrating the internet of things and bim technologies in modular integrated construction. *Automation in Construction* **126**, 103663 (2021)

- [41] Tong Fung-ling, F., Liauw Hak-ka, C.: Modular integrated construction. Buildings Department, The Government of the Hong Kong Special Administrative Region. (2024)
- [42] Heikkila, J., Silvén, O.: A four-step camera calibration procedure with implicit image correction. In: Proceedings of IEEE Computer Society Conference on Computer Vision and Pattern Recognition, pp. 1106–1112 (1997). IEEE
- [43] Scaramuzza, D., Martinelli, A., Siegwart, R.: A toolbox for easily calibrating omnidirectional cameras. In: 2006 IEEE/RSJ International Conference on Intelligent Robots and Systems, pp. 5695–5701 (2006). IEEE
- [44] Yuan, C., Liu, X., Hong, X., Zhang, F.: Pixel-level extrinsic self calibration of high resolution lidar and camera in targetless environments. IEEE Robotics and Automation Letters **6**(4), 7517–7524 (2021)
- [45] Welch, G.: An introduction to the kalman filter (1995)
- [46] Raj, T., Hanim Hashim, F., Baseri Huddin, A., Ibrahim, M.F., Hussain, A.: A survey on lidar scanning mechanisms. Electronics **9**(5), 741 (2020)
- [47] Jocher, G., Chaurasia, A., Stoken, A., Borovec, J., Kwon, Y., Michael, K., Fang, J., Yifu, Z., Wong, C., Montes, D., et al.: ultralytics/yolov5: v7. 0-yolov5 sota realtime instance segmentation. Zenodo (2022)
- [48] Sohan, M., Sai Ram, T., Reddy, R., Venkata, C.: A review on yolov8 and its advancements. In: International Conference on Data Intelligence and Cognitive Informatics, pp. 529–545 (2024). Springer
- [49] Kirillov, A., Mintun, E., Ravi, N., Mao, H., Rolland, C., Gustafson, L., Xiao, T., Whitehead, S., Berg, A.C., Lo, W.-Y., et al.: Segment anything. In: Proceedings of the IEEE/CVF International Conference on Computer Vision, pp. 4015–4026 (2023)
- [50] Arthur, D., Vassilvitskii, S.: How slow is the k-means method? In: Proceedings of the Twenty-second Annual Symposium on Computational Geometry, pp. 144–153 (2006)
- [51] Comaniciu, D., Meer, P.: Mean shift: A robust approach toward feature space analysis. IEEE Transactions on Pattern Analysis and Machine Intelligence **24**(5), 603–619 (2002)
- [52] Padilla, R., Netto, S.L., Da Silva, E.A.: A survey on performance metrics for object-detection algorithms. In: 2020 International Conference on Systems, Signals and Image Processing (IWSSIP), pp. 237–242 (2020). IEEE